CHALMERS
UNIVERSITY OF TECHNOLOGY

Production and decay properties of the lightest osmium isotopes

Citation for the original published paper (version of record):
Briscoe, A., Page, R., McCarter, A. et al (2026). Production and decay properties of the lightest osmium isotopes. Physical Review C, 113(4). http://dx.doi.org/10.1103/5rxb-bscn

(article starts on next page)

Production and decay properties of the lightest osmium isotopes

A. D. Briscoe,[1,2,*] R. D. Page,[1] A. McCarter,[1,†] J. Uusitalo,[2,1] S. Antalic,[3] D. T. Joss,[1] K. Auranen,[2] M. A. M. AlAqeel,[11,1] B. Alayed,[12,1] B. Andel,[3] H. Ayatollahzadeh,[4] H. Badran,[2] L. Barber,[5] G. Beeton,[4] M. Birova,[6] V. Bogdanoff,[2] J. G. Cubiss,[7,‡] D. M. Cullen,[5] J. Deary,[4] U. Forsberg,[2] T. Grahn,[2] P. T. Greenlees,[2] J. B. Hilton,[1,2] A. Illana,[2,§] H. Joukainen,[2,∥] D. S. Judson,[1] R. Julin,[2] H. Jutila,[2] J. M. Keatings,[4] M. Labiche,[8] M. Leino,[2] M. C. Lewis,[1] J. Louko,[2] M. Luoma,[2] I. Martel,[1,13] P. P. McKee,[4] P. Mosat,[3] S. N. Nathaniel,[1] O. Neuvonen,[2] D. O'Donnell,[4] J. Ojala,[2] C. A. A. Page,[7] J. Pakarinen,[2] P. Papadakis,[8] E. Parr,[1] J. Partanen,[2,¶] A. M. Plaza,[2,1,**] P. Rahkila,[2] E. Rey-herme,[9] P. Ruotsalainen,[2] J. Sarén,[2] J. Smallcombe,[1,††] J. F. Smith,[4] J. Sorri,[10,‡‡] C. M. Sullivan,[1] S. Szwec,[2] H. Tann,[1,2] A. Tolosa Delgado,[2] E. Uusikylä,[2] M. Venhart,[6] L. Waring,[1] and G. L. Zimba[2,§§]

[1]*Department of Physics, Oliver Lodge Laboratory, University of Liverpool, Liverpool, L69 7ZE, United Kingdom*
[2]*Accelerator Laboratory, Department of Physics, University of Jyväskylä, FI-40014 Jyväskylä, Finland*
[3]*Department of Nuclear Physics and Biophysics, Comenius University in Bratislava, 84248 Bratislava, Slovakia*
[4]*School of Computing, Engineering, and Physics Sciences, University of the West of Scotland, Paisley, PA1 2BE, United Kingdom*
[5]*Department of Physics and Astronomy, Schuster Building, The University of Manchester, Manchester, M13 9PL, United Kingdom*
[6]*Institute of Physics, Slovak Academy of Sciences, SK-84511 Bratislava, Slovakia*
[7]*School of Physics, Engineering and Technology, The University of York, York, YO10 5DD, United Kingdom*
[8]*Science and Technology Facilities Council, Daresbury Laboratory, Warrington WA4 4AD, United Kingdom*
[9]*Irfu, CEA, Université Paris-Saclay, 91191 Gif-sur-Yvette, France*
[10]*Sodankylä Geophysical Observatory, University of Oulu, FI-99600 Sodankylä, Finland*
[11]*Physics Department, Imam Mohammad Ibn Saud Islamic University (IMSIU), P.O. Box 90950, Riyadh, 11623, Saudi Arabia*
[12]*Department of Physics, College of Science, Qassim University, Buraydah, 51452, Saudi Arabia*
[13]*Faculty of Experimental Sciences, University of Huelva, 21071 Huelva, Spain*

(Received 19 December 2025; accepted 23 February 2026; published 22 April 2026)

The production of ^{159,160,161}Os and ^{159,160,161}Re was investigated in experiments performed at the Accelerator Laboratory of the University of Jyväskylä. The nuclei of interest were produced using fusion-evaporation reactions induced by beams of 275–353 MeV ^{58}Ni ions bombarding a ^{106}Cd target. The evaporation residues were separated in flight using the recoil separator MARA and implanted into a double-sided silicon strip detector, which was used to measure their decays. Cross sections for the production of these nuclides were measured and the relative population of the 8^+ isomeric states and ground states of the N=84 isotones ^{156}Hf, ^{158}W, and ^{160}Os were deduced. New decay chains assigned to ^{160}Os were identified at beam energies of 310 and 330 MeV. These findings are compared with previous studies claiming the observation of ^{160}Os and ^{156}W. The α decays of ^{161}Os were observed, confirming previous results for this nuclide and its β-decaying daughter, ^{157}W. The α-decay branch of ^{159}Re was also confirmed, but no delayed decays of this nuclide were observed that would be a signature of the β decays of the as yet unknown nuclide ^{159}Os.

DOI: 10.1103/5rxb-bscn

I. INTRODUCTION

Understanding the properties of nuclei at the boundary of the nuclear landscape is an important and topical challenge in nuclear physics research [1,2]. Information on decay energies, half-lives, and branching ratios can be extracted, even

*Contact author: adbrisco@liverpool.ac.uk
†Present address: Van Swinderen Institute for Particle Physics and Gravity, University of Groningen, Groningen, 9747AA, The Netherlands.
‡Present address: School of Physics and Astronomy, University of Edinburgh, Edinburgh EH9 3FD, United Kingdom.
§Present address: Grupo de Física Nuclear & IPARCOS, Universidad Complutense de Madrid, CEI Moncloa, E-28040 Madrid, Spain.
∥Present address: Department of Physics, Chalmers University of Technology, 412 96, Gothenburg, Sweden.
¶Deceased.
**Present address: Center for Nuclear Study, the University of Tokyo, Hirosawa 2-1, Wako, 351-0198, Saitama, Japan.
††Present address: Advanced Science Research Center, Japan Atomic Energy Agency (JAEA), Tokai, Ibaraki 319-1195, Japan.
‡‡Present address: Radiation and Nuclear Safety Authority in Finland (STUK), FI-01370 Vantaa, Finland.
§§Present address: Department of Physics and Astronomy, Louisiana State University, Baton Rouge, Louisiana 70803, USA.

in cases where only a small sample of the nuclide of interest can be produced, providing that the levels of background are sufficiently low. These measurements can be used to test the validity of theoretical models in nuclei that are very distant from the region of β stability.

A typical example is the observation of ground-state α decays of the lightest known osmium isotope, ^{160}Os, which has been claimed in two recent studies [3,4]. The reported decay energies and half-lives appear to be consistent, but there are striking differences between the observations. Most obvious is the absence of α decays from the isomeric state in ^{160}Os in Fig. 2(b) in Ref. [4], which only presents spectra correlated with subsequent proton emission from the ground state of ^{156}Ta [see Fig. 1(a)]. In contrast, in Ref. [3], 14 α-decay chains were assigned to the isomeric state in ^{160}Os, compared with 4 to its ground state. Furthermore, only two correlations were observed with ground-state proton decays of ^{156}Ta in Ref. [3], while one chain was correlated with proton decays of its isomeric state and the remaining chains were correlated with ^{156}Hf α decays following ^{156}Ta β decays. Details of these decay chains were presented in Table 1 in Ref. [3].

Although both studies employed beams of ^{58}Ni ions bombarding ^{106}Cd targets to produce the ^{160}Os nuclei in fusion-evaporation reactions, different beam energies were used. In this paper we build upon our results reported in Ref. [3] by presenting measurements performed using the same reaction over a wide range of beam energies and comparing the production rates of α-decaying ground states and isomeric states for the $N = 84$ isotones ^{156}Hf, ^{158}W, and ^{160}Os [5–8]. We confirm the decay properties of ^{161}Os and ^{157}W [9], and present a search for the β decays of the unknown nuclide ^{159}Os. We also compare the measured cross sections for ^{160,161}Os and ^{159,160,161}Re with HIVAP model calculations [10] and explore an alternative explanation for the observations presented in Ref. [4].

II. EXPERIMENTAL DETAILS

The experiments were performed at the Accelerator Laboratory of the University of Jyväskylä. The nuclei of interest were produced in fusion-evaporation reactions induced by ^{58}Ni ions of various energies bombarding a self-supporting ^{106}Cd target of 96.5% isotopic enrichment and 1 mg/cm^2 thickness. Details of the beam energies, average beam intensities and irradiation times are presented in Table I and compared with those of Ref. [4].

Light-charged particles emitted at the target position during evaporation residue formation were detected using JYTube [11], which enhanced the selectivity for weakly produced evaporation channels involving zero or only one charged particle. JYTube comprised 120 plastic scintillator detectors arranged in a hexagonal-cylindrical geometry. Each detector was 2 mm thick and was directly coupled to a silicon photomultiplier. Evaporation residues recoiling out of the target passed through a carbon foil of nominal thickness 50 μg/cm^2 mounted 10 cm downstream of the target and were transported using the recoil mass separator MARA [11] to the detector system installed at its focal plane. The ions passed through a multiwire proportional counter (MWPC) and were implanted into a double-sided silicon strip detector (DSSD).

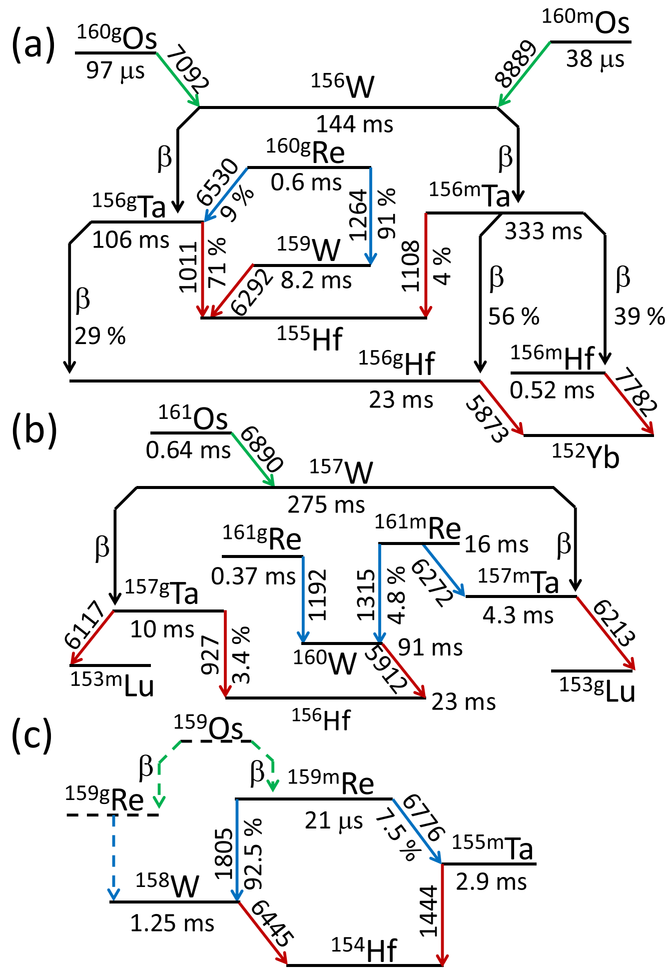

FIG. 1. Schematic diagram showing partial decay chains of (a) ^{160}Os and ^{160}Re, (b) ^{161}Os and ^{161}Re, and (c) ^{159}Re and possible decay chains of ^{159}Os. Vertical arrows indicating proton decays and diagonal arrows showing α decays are labeled with decay energies in keV. Some are also labeled with branching ratios. Other branching ratios are either close to 100% or can be deduced from the value for the competing decay branch. Half-lives of levels are also given. Decays of Os and Re nuclei are highlighted in green and blue, respectively, while the decays used to identify them in the correlation analysis are highlighted in red. Dashed lines and arrows indicate decays and states that have not yet been observed. Data are taken from Refs. [3,5,6,9,16,18,21,22] and the present work.

The energy signal in the DSSD and the time of flight between the MWPC and the DSSD was used to distinguish evaporation residues from beam-like particles. The DSSD was 300 μm thick and had an active area of 128 mm × 48 mm. The strips on its front and back surfaces were orthogonal and the strip pitch of 0.67 mm on both faces provided 13 824 independent pixels. This high degree of segmentation allowed for clean correlations even when decay chains involved comparatively slow β decays, as well as long maximum correlation time intervals, which are important when measuring half-lives. The DSSD energy thresholds were set at ≈100 keV to allow the observation of β-decay and conversion-electron signals. The DSSD was calibrated using the implanted α activities of

TABLE I. Details of the front-of-target ^{58}Ni beam energies, average beam intensities in particle nA, ^{106}Cd target thicknesses and irradiation times for the reactions studied in the present work. The corresponding details from Ref. [4] are presented in the bottom line.

Energy (MeV)	Intensity (pnA)	Thickness (mg/cm^2)	Time (h)
275	2.7	1.0	11
293	2.9	1.0	6
310	3.6	1.0	285
330	2.7	1.0	70
338	2.7	1.0	192
353	2.8	1.0	28
335	10	0.4	163

^{150,151}Dy, ^{152}Er, ^{155}Lu, ^{156}Hf, and ^{158}Ta nuclei. An energy resolution of ≈40 keV FWHM was obtained. The minimum time difference between successive signals in a given strip was 8 μs.

An array of eight detectors was mounted around the perimeter of the DSSD in the upstream direction for the data collected at 310 MeV. These detectors formed the walls of a silicon "box" while the DSSD formed the base. These box detectors were used to measure the residual energies of α particles and protons emitted from within the DSSD in the upstream direction, depositing only part of their energy. The energies of these escaping particles could be reconstructed by summing the energies registered in the DSSD and box detectors, albeit with a reduced energy resolution of ≈100 keV FWHM and a low-energy tail that extended more than 1 MeV below the sum peak.

Six of the box detectors had active areas of 50 mm × 50 mm, segmented into four quadrants and were 500 μm thick. These were mounted in two groups of three around the ends of the DSSD. To complete the array, the other two box detectors were mounted centrally above and below the DSSD, between the two groups of square box detectors. These two detectors each measured 25 mm × 75 mm, were 500 μm thick and segmented into two elements. The box detectors were assembled on a frame to complete the four box walls with their downstream edges aligned.

High-energy light ions arriving at the MARA focal plane that "punched through" the DSSD were identified using two 500-μm-thick silicon detectors mounted directly behind the DSSD. These detectors had an active area of 50 mm × 70 mm and allowed the background arising from these particles in the DSSD to be suppressed, in addition to vetoing signals from high-energy β decays from implanted nuclei.

All detector signals were passed to the triggerless data acquisition system and time stamped with a precision of 10 ns [12]. The data were analysed using the GRAIN [13] software package.

III. RESULTS

A. Decay of ^{160}Os

The α-particle energy and half-life we previously reported for the isomeric state in ^{160}Os were 8890(10) keV and 41^{+15}_{-9} μs [3], while the corresponding values reported for its ground state were 7092(15) keV and 97^{+97}_{-32} μs in Ref. [3], and 7080(26) keV and 201^{+58}_{-37} μs in Ref. [4]. Figure 2 shows α-particle energies plotted against the natural logarithm of the time they were observed after the implantation of an ion into the same DSSD pixel. The α-decay peaks of the high-spin isomeric states in ^{155}Lu, ^{156}Hf, and ^{158}W are visible in all spectra at energies of 7.4, 7.8, and 8.3 MeV, respectively. As well as having larger maximum production cross sections, these nuclides can all be produced at lower beam energies by evaporation channels involving α particles, with individual nucleon evaporation dominating at higher beam energies. Consequently, they are observed over a wider range of beam energies than ^{160}Os, which can only be produced by neutron evaporation in this reaction. The 8.6-MeV α decays of the 6 μs isomeric state in ^{158}Ta [14,15] are also visible in Figs. 2(c)–2(f). Their α-particle energy distribution is broadened because they occurred so soon after the ions were

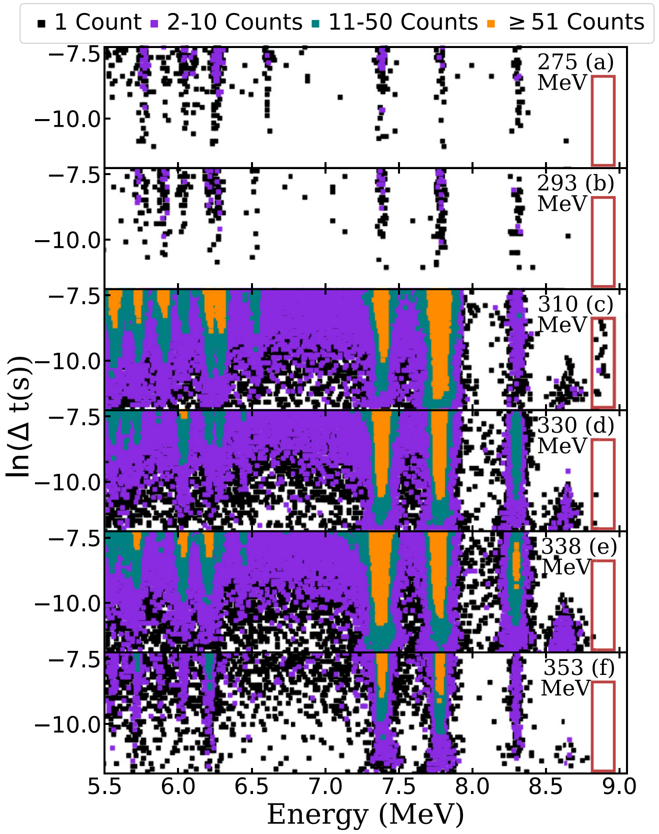

FIG. 2. Energies of α decays plotted against the natural logarithm of the time interval between the decay and the preceding ion implantation into the same DSSD pixel. The number of signals recorded in JYTube in association with the implanted ions was restricted to be fewer than 2. The spectra were measured at front-of-target beam energies of (a) 275 MeV, (b) 293 MeV, (c) 310 MeV, (d) 330 MeV, (e) 338 MeV, and (f) 353 MeV. The red rectangles indicate where α decays of the isomeric state in ^{160}Os could appear. The α decays of the the high-spin isomeric states in ^{155}Lu, ^{156}Hf, ^{158}W, and ^{158}Ta are at energies of 7.4, 7.8, 8.3, and 8.6 MeV, respectively.

TABLE II. Data recorded for additional candidate ^{160}Os decay chains to those reported in Ref. [3]. E_n is the energy of the nth signal in the chain and t_n is its time after the preceding signal in the same DSSD pixel. The times t_n have not been corrected for the 8 μs minimum observation time. However, the half-lives presented in the text have had a correction for this applied. The JYTube fold is the number of coincident signals observed in JYTube in association with the evaporation residue for each chain and was required to be no more than one for chains to be considered as candidates for ^{160}Os, which was produced via the 4n evaporation channel. Reconstructed energies of α particles that escaped the DSSD and were stopped in the box detectors are indicated by italics. The energies of signals below 500 keV were calibrated using conversion electrons from an external ^{133}Ba source rather than implanted α activities. The superscript letters denote the assignments to decays following ^{160}Os candidates where they could be identified. Chains one and three are interpreted as decays of the high-spin isomeric state in ^{158}Ta [14,15], while the remaining chains with numbers in the first column in bold font are interpreted as decays of ^{160}Os.

Chain #	Assignment	E_1 (keV)	t_1 (μs)	E_2 (keV)	t_2 (ms)	E_3 (keV)	t_3 (ms)	E_4 (keV)	t_4 (ms)	E_5 (keV)	t_5 (ms)	JYTube Fold	Beam Energy (MeV)
1	^{158m}Ta	8839	10	140	102	5323[a]	103	4245	18 043	—	—	1	330
2	^{160m}Os	8850	27	225	190	1660[b]	708	237	56	4795[c]	17 691	0	330
3	^{158m}Ta	8830	13	173	7689	5283[a]	6	5107	8279	—	—	1	338
4	^{160m}Os	8905	76	233	556	5878[d]	231	318	23 393	4816[c]	10 648	0	310
5	^{160m}Os	8885	75	469	200	*5619*[e]	820	—	—	—	—	0	310
6	^{160m}Os	8886	65	*5117*[f]	642	4801[c]	10 895	—	—	—	—	0	310
7	^{160m}Os	8855	13	*7749*[g]	206	5091	5609	261	1175	—	—	0	310

[a]α decay of ^{154}Yb.
[b]α decay of ^{156}Hf with partial energy deposition.
[c]α decay of ^{152}Er.
[d]α decay of ^{156g}Hf.
[e]α decay of ^{156g}Hf with partial energy deposition, with 1499 and 4120 keV in the DSSD and box, respectively.
[f]α decay of ^{156g}Hf with partial energy deposition, with 1223 and 3894 keV in the DSSD and box, respectively.
[g]α decay of ^{156m}Hf with partial energy deposition, with 1206 and 6543 keV in the DSSD and box, respectively.

implanted and the short half-life leads to a partial pile up with the preceding implantation signal.

As can be seen in Figs. 2(a), 2(b), and 2(f), no α decays of the 8.9-MeV isomeric state in ^{160}Os were observed at 275, 293, or 353 MeV. The spectrum measured at 310 MeV shown in Fig. 2(c) was obtained from the same data set that was used in Ref. [3]. In addition to the 14 events at 310 MeV we reported in Ref. [3], four new candidate events around 8.9 MeV were identified [see Fig. 2(c)], along with two at 330 MeV [Fig. 2(d)] and one at 338 MeV [Fig. 2(e)]. To determine whether or not they are decays of ^{160}Os it is necessary to analyse their subsequent decays. Figures 3(a)–3(c) show energy-energy correlation matrices for successive decays in the DSSD obtained at beam energies of 310, 330, and 338 MeV, respectively, and full details of the new candidate decay chains are presented in Table II. Since ^{156}W, the daughter of ^{160}Os α decays, undergoes β decay, correlations must be sought with proton decays of ^{156}Ta or α decays of the ground state and isomeric state of ^{156}Hf populated in the β decays of ^{156}Ta; see Fig. 1(a).

Chains 1 and 3 are interpreted as α decays of the high-spin isomeric state in ^{158}Ta ($E_\alpha = 8.6$ MeV, $t_{1/2} = 6$ μs) [14,15], because these α decays appear to be followed by a β decay, then a 5331-keV α decay of ^{154}Yb [17]. Chain 2 was measured at beam energy of 330 MeV and is interpreted as an α decay of the isomeric state in ^{160}Os, followed by an α decay of ^{156}Hf that escaped the DSSD without depositing its full energy, then a 4804-keV α decay of ^{152}Er [17]. One of the two intervening β decays was detected between each pair of α decays. These assignments are consistent with the number of charged particles registered in JYTube in each case.

Details of decay chains following the ^{160}Os isomer α decays obtained at a beam energy of 310 MeV that were not presented in Ref. [3] are also included in Table II. In chain 4 the ground-state α decay of ^{156}Hf occurred within 8 μs of a signal in the MWPC, which is why it was not included in the analysis in Ref. [3]. However, the MWPC position was outside the acceptance of the DSSD and therefore this signal had no spatial correlation with the α decay. In chains 5–7, one of the subsequent α decays was observed in coincidence with a signal in a box detector. The full α-particle energies reconstructed by adding the energy signals from the DSSD and box detector allow these decays to be identified as those of the ground state (chains 5 and 6) or isomeric state (chain 7) of ^{156}Hf. In chains 4 and 6, the ^{156}Hf α decay was observed to be followed by an α decay of ^{152}Er. These five additional decay chains from Table II that were assigned to the isomeric state of ^{160}Os allow an updated value for its half-life to be determined. Combining data for the new chains with those already presented in Ref. [3] leads to a revised α-particle energy of 8889(10) keV and half-life of 38^{+12}_{-7} μs. These more precise values do not alter any conclusions of Ref. [3].

There were five other short-lived events having energies and time differences compatible with α decays of the isomeric state in ^{160}Os. However, the subsequent decay events in these chains involved α particles that escaped from the DSSD, depositing only part of their energy without being registered in the box detectors. It was therefore not possible to reconstruct their full energy and determine which decay path they followed, so these five chains are not considered further below.

The region of the energy spectra around 7.1 MeV, where the ground-state α decays of ^{160}Os should appear, is subject to

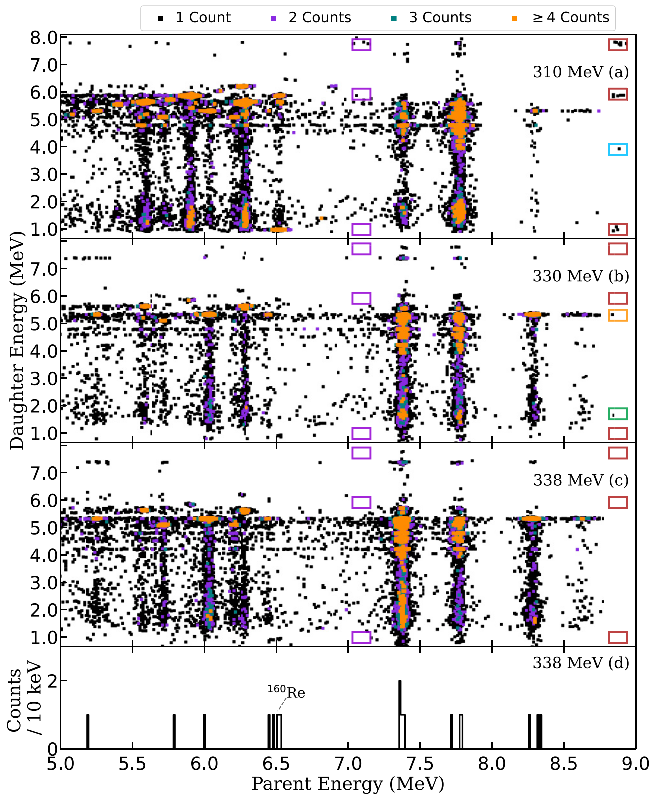

FIG. 3. Energy-energy correlation matrices for two consecutive decay events where the first decay occurred less than 1.1 ms after an ion in the same detector pixel and was followed within 1.75 s by the second decay. The spectra were measured at beam energies of (a) 310 MeV, (b) 330 MeV, and (c) 338 MeV. Events observed in coincidence with a signal in a box detector are excluded in (a). The rectangles show regions where α decays of the ground state (purple) and isomeric state (red) of ^{160}Os are expected from correlations with α decays of ^{156}Hf at 5.9 and 7.8 MeV, or proton decays of ^{156}Ta at 1.0 and 1.1 MeV. The event highlighted by the blue rectangle is one of the five chains that were excluded from the analysis because the subsequent decays involve escaping α particles that could not be used to provide a definitive assignment to ^{160}Os. The orange and green rectangles highlight the events from chains 1 and 2, respectively. Note that the energy scales are valid only for α decays and give apparent proton energies that are ≈40 keV too low. (d) Energy spectrum of α decays observed in the 338-MeV data within 700 μs of an ion implantation in the same DSSD pixel and followed by a decay having an energy consistent with proton decay of the ^{156}Ta ground state within 1.2 s. In all spectra no more than one signal was observed in JYTube in association with each evaporation residue and the minimum energy threshold was set in the analysis to exclude β-decay events from these correlations.

background from α particles from higher-energy decay lines that do not register their full energy in the DSSD. It is therefore necessary to correlate with subsequent decays to extract the ^{160}Os α decays from this background. In Figs. 3(a)–3(c), the first decay was required to occur within 1.1 ms after an ion implantation and be followed within 1.75 s by the second decay, with all signals in the same detector pixel. No additional candidate decays to the four reported in Ref. [3] are visible in Fig. 3 in any regions where correlations would be expected. However, it can be seen in Fig. 3 that there is little or no background in the regions of the matrices where the correlated ^{160}Os ground-state α decays are expected, particularly for the α decays of the isomeric state in ^{156}Hf.

To provide a direct comparison with Fig. 2(b) in Ref. [4], Fig. 3(d) shows the energy spectrum obtained from the 338-MeV data set of α decays observed within 700 μs of an ion implantation in the same DSSD pixel and followed within 1.2 s by a decay having an energy consistent with proton decay of the ^{156}Ta ground state. There is less background evident in Fig. 3(d) than in the spectrum in Ref. [4], which used the same maximum time intervals. This reflects the cleaner correlations that can be achieved with the more highly segmented silicon detector used at the focal plane of MARA and the selection provided by JYTube. In contrast to the ≈20 events claimed in Ref. [4] there are no events observed around 7.1 MeV, despite the similar beam energy and comparable beam dose.

The new ^{160}Os decay chains in Table II can be used in measuring the half-life of ^{156}W, provided that the subsequent decay paths are unambiguous. The time differences between the ^{160}Os α decays and following ^{156}Hf isomer α decays of chains 2 and 7, taking into account the intervening β decays, were combined with the data from Ref. [3] to obtain a more precise value of 144^{+48}_{-30} ms.

B. Decay of ^{161}Os

The reported α-particle energy and half-life from the only previous study of ^{161}Os were 6890(12) keV and 640(60) μs [9]. As with the ground-state α decays of ^{160}Os, correlations with subsequent decays were required to extract ^{161}Os α decays from the background. The correlation analysis in the case of ^{161}Os is slightly simpler: its daughter, ^{157}W, β decays with a half-life of 275(40) ms [9], feeding both low-lying α-decaying states in ^{157}Ta; see Fig. 1(b). Evidence for the correlated α decays of ^{161}Os was observed in the data collected at beam energies of 275, 293, and 310 MeV; see Fig. 4. The events at 6894(13) keV were found to be correlated with both the ground state of ^{157}Ta and its low-lying isomeric state, confirming the previous assignment to ^{161}Os.

The half-life of ^{161}Os was measured from the present data to be 610^{+155}_{-105} μs. A half-life of 360^{+110}_{-80} ms was determined for ^{157}W from the time differences between the α decays of ^{161}Os and ^{157}Ta, taking into account the half-lives of the ^{157}Ta states. These values are consistent with those reported in Ref. [9], which also presented evidence for fine structure in the α decay of ^{161}Os. A single event at an energy of 6582 keV was found in the 310-MeV data to be correlated with a ground-state α decay of ^{157}Ta; see Fig. 4(c). This is in agreement with the energy of 6580(30) keV reported for fine-structure α decays of ^{161}Os and the number of counts is compatible with the previously reported branching ratio of $5.5^{+3.1}_{-2.2}$ % [9].

C. Search for decays of ^{159}Os

The present data were searched for evidence of the unknown nuclide ^{159}Os, which is expected mainly to undergo β decay with a predicted half-life of 145 ms, because Q values for α decay drop for neutron numbers just below $N = 84$ [19]. Assuming its β-decay pattern resembles those of its isotones

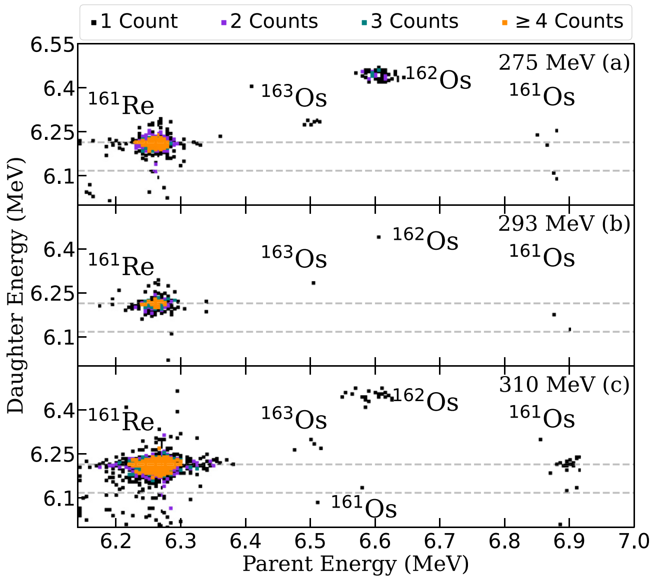

FIG. 4. Energy-energy correlation matrices for two consecutive α-decay events where the first decay was a maximum of 6.4 ms after an ion in the same detector pixel and followed within 2.8 s by the second decay. An additional condition has been applied requiring that no more than one signal was observed in JYTube in association with the evaporation residue [3]. The spectra were measured at beam energies of (a) 275 MeV, (b) 293 MeV, and (c) 310 MeV. Groups identified as decays of $^{161-163}$Os and ^{161}Re correlated with their respective subsequent α decays are labeled. The dashed horizontal lines indicate the expected energies of ^{157}Ta α decays.

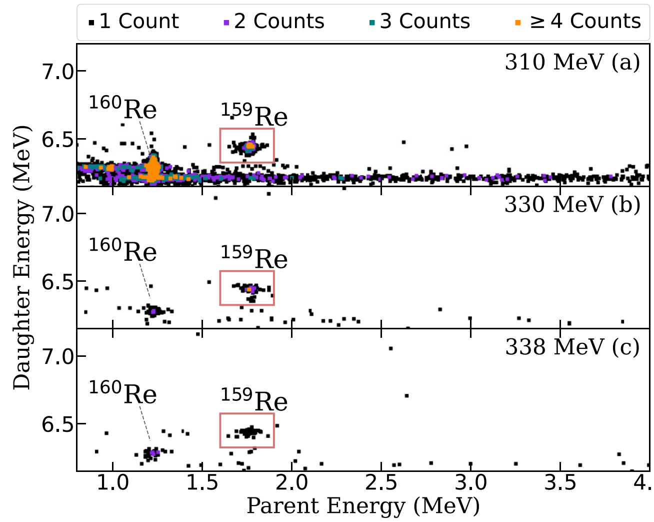

FIG. 5. Energy-energy correlation matrices for two consecutive decay events where the first decay occurred less than 10 s after an ion implantation in the same detector pixel and was followed within 12.5 ms by the second decay. No more than two signals were observed in JYTube in association with the evaporation residue. The spectra were measured at beam energies of (a) 310 MeV, (b) 330 MeV, and (c) 338 MeV. Groups identified as proton decays of ^{159}Re and ^{160}Re correlated with their daughter α decays are labeled.

^{155}Hf [20] and ^{157}W [9], one would expect both the $\pi h_{11/2}$ isomeric state and the $\pi s_{1/2}$ ground state of ^{159}Re could be populated via intermediate states in the β decay; see Fig. 1(c). The isomeric state of ^{159}Re has been observed to undergo proton emission [21] and α-particle emission [22] with a half-life of 21(4) µs. Its ground state has yet to be observed, but has an estimated proton-decay Q value of 1686(37) keV and half-life of around 17 ns [23]. Whichever state in ^{159}Re is populated, its decay will appear to be delayed because of the comparatively slow β decay of ^{159}Os.

The decays of the isomeric state of ^{159}Re were observed at beam energies of 310, 330, and 338 MeV. Proton decays of ^{159}Re were identified through correlations with subsequent α decays of the ground state of ^{158}W [5–8]. Figure 5 shows energy-energy correlation matrices of proton decays occurring within 10 s of an ion being implanted into the same DSSD pixel that were followed within 12.5 ms by an α decay. It can be seen that there is a single group corresponding to the 1805-keV proton emission from the isomeric state in ^{159}Re, but no evidence for a second peak ≈130 keV lower in energy that could correspond to decays of its ground state. Owing to the expected short half-life of the ground state of ^{159}Re it is likely that its proton-decay signals will pile up with the signals from the β decays of ^{159}Os and appear spread across a range of higher energies. However, there is no clear sign of this in the spectra either.

Figure 6 shows spectra featuring 6776(26)-keV ^{159}Re α decays followed by proton decays of ^{155}Ta ($E_p = 1444(15)$ keV, $t_{1/2} = 2.9^{+1.5}_{-1.1}$ ms) [22]. Timing conditions requiring that the first decay occurred within 10 s of an ion being implanted into the same DSSD pixel and the second followed within a

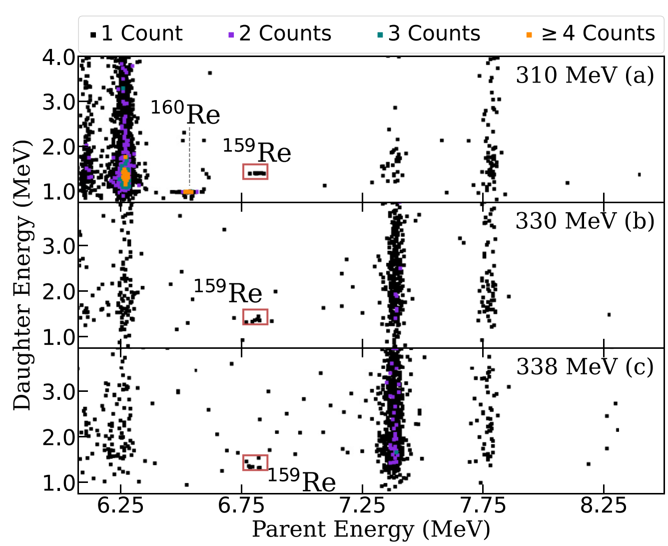

FIG. 6. Energy-energy correlation matrices for two consecutive decay events where the first decay occurred less than 10 s after an ion implantation in the same detector pixel and was followed within 15 ms by the second decay. No more than two signals were observed in JYTube in association with the evaporation residue. The spectra were measured at beam energies of (a) 310 MeV, (b) 330 MeV, and (c) 338 MeV. Groups identified as α decays of ^{159}Re and ^{160}Re correlated with their daughter proton decays are labeled.

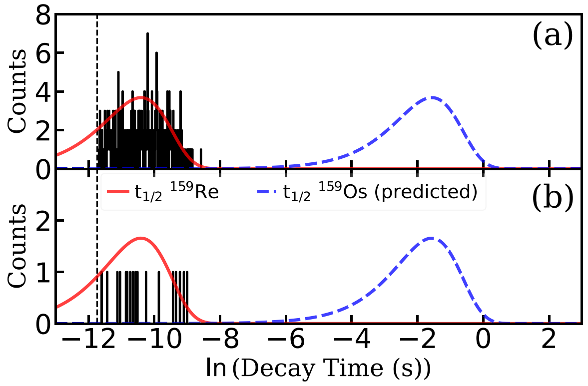

FIG. 7. Natural logarithm of the time interval between the implantation of an ion into a DSSD pixel and subsequent (a) ^{159}Re proton decays correlated with ^{158}W α decays, and (b) ^{159}Re α decays correlated with ^{155}Ta proton decays. Time distributions for the literature value of the half-life of ^{159}Re [21,22] and the predicted half-life of the β decay of ^{159}Os [19] are shown by the solid red and dashed blue curves, respectively. The vertical dashed lines show the minimum time response of 8 μs following ion implantation.

further 15 ms were applied. These spectra provide the first confirmation of the α-decay branch of ^{159}Re [22].

The natural logarithm of the time after ion implantation of the ^{159}Re decays observed at all beam energies is shown in Fig. 7 and compared with the expected time distributions for the decays of ^{159}Re and ^{159}Os. In total, the decays of 341 ^{159}Re nuclei were identified in the present work, but all of them occurred within 190 μs and were therefore consistent with the reported half-life of 21(4) μs [21,22]. Furthermore, no β-decay signals were observed between the ion implantation and ^{159}Re decay events. On this basis we conclude that there is no evidence in the present data for the observation of decays of ^{159}Os, presumably because the production cross section for ^{159}Os is at least a factor of 100 lower than that for ^{159}Re.

IV. DISCUSSION

In Ref. [3], the isomeric state in ^{160}Os was found to be populated more strongly than the ground state. In the present work, the additional chains assigned to ^{160}Os are all decays of the isomeric state. This relative population in ^{160}Os is similar to those of the corresponding states in its even-even $N = 84$ isotones ^{156}Hf and ^{158}W in fusion-evaporation reactions [5,7,8]. This can be seen in Fig. 8(a) which compares the percentages of ions in the isomeric state measured for ^{160}Os at 310 MeV with those of ^{156}Hf and ^{158}W over a range of beam energies. The isomeric ratio for ^{160}Os was calculated from the 23 isomer decays observed in Fig. 2(c) and the four ground-state decays from Fig. 3(a), with corrections applied for detection efficiency. A virtually identical isomeric ratio was found using instead the number of correlated decay chains and applying efficiency corrections. The isomeric ratios are comparable for all three isotones with an average value of around 80%. Yang *et al.* state that their ^{160}Os peak comprised ∼20 counts. The data point plotted in green in Fig. 8(a) is based on this number and noting that there is a single count close to 8.9 MeV in their Fig. 2(b) which could be a ^{160}Os

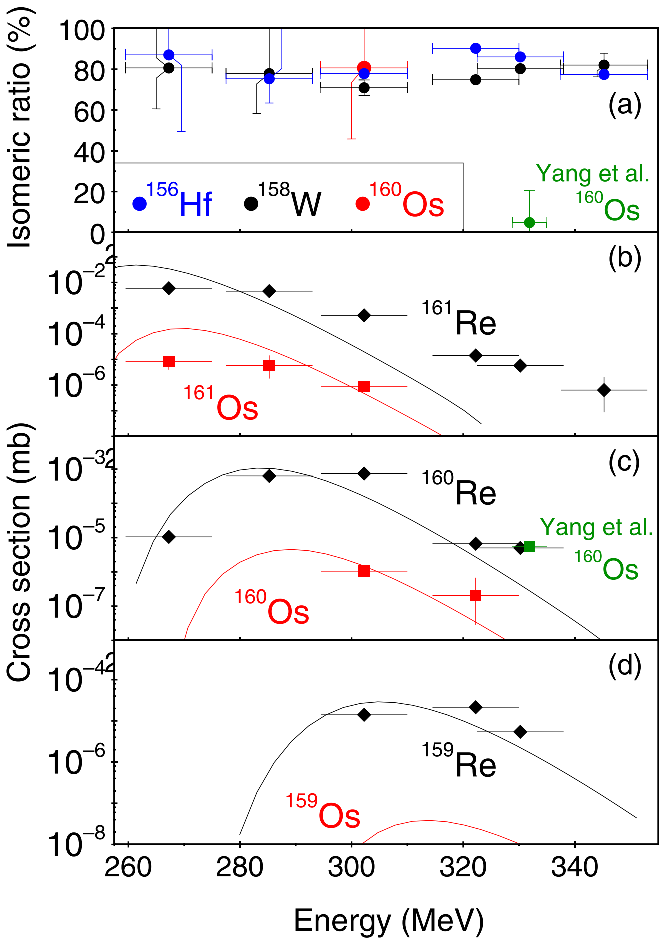

FIG. 8. (a) Percentage of ^{156}Hf, ^{158}W, and ^{160}Os nuclei implanted into the DSSD that were in the isomeric 8^+ state for the different beam energies used in the present work. Measured cross sections compared with values calculated using the statistical-model code HIVAP [10] for the production of (b) ^{161}Os and ^{161}Re, (c) ^{160}Os and ^{160}Re, and (d) ^{159}Os (calculations only) and ^{159}Re in the fusion-evaporation reaction ^{58}Ni + ^{106}Cd. Calculations and measurements for Os (Re) isotopes are shown by the red (black) curves and symbols, respectively. Statistical uncertainties are shown where they are larger than the symbol size. Measured values are plotted at the estimated beam energy at the center of the target and the horizontal bar indicates the range of ^{58}Ni ion energies sampled in each measurement as they passed through the target. The isomeric ratio and cross section for ^{160}Os deduced from the paper by Yang *et al.* [4] are shown in green.

isomer α decay. Clearly the observations presented in Ref. [4] implying an isomeric ratio at a beam energy of 335 MeV that is close to 0% do not fit these systematics.

Total production cross sections for ^{160,161}Os and $^{159–161}$Re were estimated at each beam energy from the combined yields of all observed proton- and α-decaying states for each nuclide and the results are shown in Figs. 8(b)–8(d). The cross sections are plotted at the estimated beam energy at the centre of the target, with the horizontal lines indicating the spread of ^{58}Ni beam energies in the target. A MARA transmission efficiency of 40(10) % was assumed in all cases and its uncertainty generally dominated the overall uncertainty in the cross sections. Corrections were applied for branching ratios, time gates, and the fraction of decay events depositing their full energy in the DSSD. The cross sections for the production of ^{160}Os at 310 and 330 MeV were estimated to be 1.0(3) nb and $0.2^{+0.5}_{-0.2}$ nb, respectively.

The estimated cross sections were compared with values calculated using the statistical-model code HIVAP [10]. In these calculations, the rotating liquid-drop model [24] contribution of the total fission barrier was scaled down by a factor of $C_f = 0.53$. Lowering the fission barrier height has been found to improve the agreement of calculated cross sections with measured values for neutron-deficient nuclei [25]. The measured excitation functions appear to be slightly broader than the calculated ones, although use of the thick targets in the experiments makes direct comparisons difficult because energy losses and scattering within the target leads to broadening. In addition, isotopic impurities at the few % level in the target could lead to enhanced production at higher beam energies from their heavier, less fissile compound nuclei.

The cross section of $5.4^{+1.2}_{-1.0}$ nb estimated for the ground state of ^{160}Os in Ref. [4] is also plotted in Fig. 8(c). This value appears to be anomalously high compared with the values measured in the present work at beam energies of 310 and 330 MeV, and the trends of the HIVAP calculations. The calculated excitation functions and the measured cross sections for ^{160}Re plotted in Fig. 8(c) suggest that the beam energy of 335 MeV employed in Ref. [4] was not optimal for producing $A = 160$ isobars.

The nonobservation of any α decays assigned to ^{160}Os in Fig. 2(e) or Fig. 3(c) leads to an upper limit on its production cross section at 338 MeV of 0.2 nb for an 84% confidence level [26]. The cross section reported in Ref. [4] is incompatible with this upper limit. At this beam energy, the ^{58}Ni ions lost around 15 MeV traversing the target, so their spread of energies fully covered the corresponding energy spread of ^{58}Ni ions in the thinner target used in Ref. [4]. Furthermore, the cross sections for producing the osmium isotopes shown in Fig. 8 are systematically lower by at least a factor of 100 compared with their rhenium isobars at any given beam energy, except for the cross section reported in Ref. [4] for ^{160}Os which is comparable to the value measured here for ^{160}Re.

The number of ground-state ^{160}Os α decays claimed in Ref. [4] does not seem to be compatible with the absence of its isomer α decays or the cross sections measured in the present work. Below we show that the apparent peak attributed to the ground state of ^{160}Os can be understood as a statistical fluctuation of the background, while the half-lives for ^{160}Os and its daughter ^{156}W reported in Ref. [4] may be fully explained as random correlations of events from longer-lived activities.

In Ref. [4] the analysis was restricted to correlations with subsequent proton emission from the ground state of ^{156}Ta. A difficulty arises because the proton-decay peak is in a region of the spectrum where there can be background originating from α particles that do not deposit their full energy. In Fig. 3(c) showing the data collected at a beam energy of 338 MeV, which is the closest match to that used in Ref. [4], it can be seen that the escaping α-particle energy distributions of events following α decays of the isomeric states in ^{155}Lu, ^{156}Hf, and ^{158}Ta extend below 1 MeV. This explains why in Ref. [4] it was necessary to compare with the background spectrum shown in Fig. 2(c) of that work. Yang *et al.* state that there was too much background in their spectra when correlating with the α decays of the ground state of ^{156}Hf that is populated by the 29% β-decay branch of the ^{156}Ta ground state [16]. However, there is no discussion of correlations with the α decays of the isomeric state of ^{156}Hf, which account for half of the ^{160}Os decay chains presented in Table 1 in Ref. [3].

TABLE III. Upper and lower limits for different confidence level intervals for the Poisson signal mean μ for a total of 20 observed events with mean background levels b of 13 and 14 events. The values are taken from Tables III, V, VII, and IX of Ref. [27].

Confidence	Lower limit		Upper limit	
level (%)	$b = 13$	$b = 14$	$b = 13$	$b = 14$
68	2.91	2.12	12.30	11.30
90	1.48	0.53	15.52	14.52
95	0.25	0.00	17.33	16.33
99	0.00	0.00	21.32	20.32

The experimental conditions for the reactions studied in the present work were comparable to those given in Ref. [4], although there is less background in our correlated energy spectra shown in Fig. 3. The inconsistencies with the present data raise the question: is the “peak” in Fig. 2(b) in Ref. [4] real? The regions of that spectrum where 20 counts can be identified have corresponding levels of 13 or 14 counts in the background spectrum shown in Fig. 2(c) of Ref. [4]. With this level of background, observing 20 counts could be an upward statistical fluctuation within 2 standard deviations [26]. Alternatively, one can use the calculated confidence intervals of Ref. [27] presented in Table III, which are based on a unified approach to the classical statistical analysis of small signal levels in the presence of background. All 20 counts can be considered to be compatible with a statistical fluctuation in the background b when the lower limit on the Poisson signal mean μ becomes zero. This happens for a confidence level between 95% and 99% for $b = 13$, and between 90% and 95% for $b = 14$. The statistical significance of the peak claimed in Ref. [4] therefore does not constitute conclusive proof of the observation of ^{160}Os. The apparent agreement of the energy with that reported in Ref. [3] could be purely coincidental.

With the observed level of background and using the methodology of Ref. [27], one can also evaluate the probability that all 20 events could really have been from the “peak” activity and none of them were from the expected background. In this case the upper limit on μ needs to be at least 20, which can be excluded with more than 95% confidence for both $b = 13$ and 14 (see Table III). Even if some of the events in the “peak” were genuine ^{160}Os ground-state α decays, this still raises questions regarding the half-life of 201^{+58}_{-37} μs reported for ^{160}Os in Ref. [4]. This value was obtained using the maximum likelihood method [26], which estimates the mean lifetime as the arithmetic mean of the individual decay times t_n at which events were observed, provided the observation period is not restricted. From the uncertainties in the reported half-life one can deduce that 20 events were used in the analysis, which matches the number of ^{160}Os events claimed in the energy spectrum that contained events occurring between 30 and 700 μs after the implantation of an ion [4]. Assuming this time interval without correcting for its finite duration, a half-life of 230 μs is expected for any activity having a long half-life. The half-life reported in Ref. [4] is consistent with this expected value for background.

A likely source of longer-lived background activity is from higher-energy α emitters, where some of the charge was not collected, resulting in a tail of lower-amplitude signals. The α-decaying isomeric states of ^{155}Lu and ^{156}Hf are plausible candidates for this, being strongly produced in this reaction; see Fig. 2. Applying the maximum likelihood method without any correction to events in the ^{155}Lu peak occurring 30 - 700 μs after an ion implantation in the data collected at 310 MeV gives apparent half-lives of 231(2) μs for ^{155}Lu and 219(2) μs for ^{156}Hf. These values are consistent within uncertainties with 201^{+58}_{-37} μs reported for ^{160}Os in Ref. [4] but are in clear disagreement with the accepted values of 2.71(3) ms for ^{155}Lu and 520(10) μs for ^{156}Hf that have been measured independently at several laboratories [5]. The slightly shorter apparent half-life for ^{156}Hf compared with ^{155}Lu reflects the shorter actual half-life of this nuclide.

Yang *et al.* do not provide details of whether any correction was applied for the finite measurement interval, or how any correction was made for the random background component that would be expected from Fig. 2(c) in Ref. [4].

If the ^{160}Os peak claimed in Ref. [4] is a fluctuation in the background from higher-energy α decays, then its "daughter" decays are likely to be randomly correlated escaping α particles, rather than proton decays of ^{156}Ta. It follows that the half-life reported there for the β decay of ^{156}W will not be correct either. The maximum time difference between ^{160}Os decay candidates and ^{156}Ta proton decays used to produce the spectra in Ref. [4] was 1.2 s. If this time interval was used to determine the half-life of ^{156}W and the decay chains were from background, then one would expect a value of 310 ms using the method of Ref. [26], after adjusting for the 106-ms half-life of the ^{156}Ta ground state. This value from background is compatible with the half-life of 291^{+86}_{-61} ms reported in Ref. [4]. Although one cannot be sure from the information provided whether this was actually done, it does serve to illustrate how such a half-life could result from random correlations of the background. For comparison, the updated half-life combining data from Ref. [3] and the present work is 144^{+48}_{-30} ms for ^{156}W. This half-life was deduced from decay chains with much longer maximum correlation times than 1.2 s, with some chains spanning tens of seconds (see Table II and Table 1 in Ref. [3]).

Finally, in our previous paper [3] we reported a reduced α-decay width for the ground state of ^{160}Os of 60(30) keV using the method of Ref. [28]. This value is consistent within uncertainties with the systematic trends for $N = 84$ isotones and does not support the claim in Ref. [4] of enhanced stability of the $N = 82$ shell closure for heavier elements. Future experiments with low-background spectra having higher statistics are required to determine whether any such effect really exists and to improve upon the present unsuccessful search for β decays of ^{159}Os.

V. SUMMARY

The production of ^{160,161}Os and $^{159–161}$Re in fusion-evaporation reactions induced by beams of ^{58}Ni ions bombarding isotopically enriched ^{106}Cd targets has been investigated. The production and α decays of ^{160}Os nuclei cast doubt on the claims made in Ref. [4] regarding the decay of its ground state. In particular, the observation of only ground-state α decays of ^{160}Os would be at odds with measured isomeric ratios; the cross section reported is anomalously high when compared with excitation functions for the lightest Os and Re isotopes; and the half-life is consistent with what would be expected for longer-lived background. It seems likely that the observed "peak" was a fluctuation in the background.

If the assignment to ^{160}Os in Ref. [4] was incorrect, then so too was the identification of its daughter, ^{156}W. The half-life reported for the β decay of ^{156}W is also consistent with expectations from a plausible background scenario. In contrast, additional ^{160}Os decay chains to those we reported in Ref. [3] were presented in this paper and support the conclusions of our earlier study.

The decay properties of ^{161}Os and ^{157}W were confirmed, but no decay chains that could be assigned as β decays originating from ^{159}Os were identified. However, ^{159}Os should be observable using the methods employed in this work, which also provide a possible approach for identifying proton emission from the very short-lived ground state of ^{159}Re.

ACKNOWLEDGMENTS

Financial support for this work has been provided by the United Kingdom Science and Technology Facilities Council (STFC) through Grants No. ST/P004598/1, No. ST/V001027/1, No. ST/Y000242/1, and No. ST/V001035/1; the EU 7th Framework Programme "Integrating Activities—Transnational Access," Project No. 262010 (ENSAR); by the Slovak Research and Development Agency (Contract No. APVV-22-0282) and Slovak Grant Agency VEGA (Contract No. 1/0019/25); and by the Academy of Finland under the Finnish Centre of Excellence Programme 2012–2017 (Nuclear and Accelerator Based Physics Programme at JYFL). T.G. acknowledges the support of the Academy of Finland, Contract No. 131665. J.P. and S.S. acknowledge the Academy of Finland (Finland) Grant No. 307685. The authors express their gratitude to the technical staff of the Accelerator Laboratory at the University of Jyväskylä for their support. The authors also thank Paul Morrall of Daresbury Laboratory for preparation of the Cd targets and to the GSI target laboratory for providing the C foils, which are highly appreciated.

DATA AVAILABILITY

The data that support the findings of this article are not publicly available. The data are available from the authors upon reasonable request.

[1] M. Thoennessen, *The Discovery of the Isotopes* (Springer International Publishing, Cham, Switzerland, 2016).

[2] M. Thoennessen and A. Gade, Isotope facilities aim to complete the nuclear chart, Nat. Phys. **20**, 1844 (2024).

[3] A. D. Briscoe, R. D. Page, J. Uusitalo, D. T. Joss, M. A. M. AlAqeel, B. Alayed, B. Andel, S. Antalic, K. Auranen, H. Ayatollahzadeh, *et al.*, Decay spectroscopy at the two-proton drip line: Radioactivity of the new nuclides ^{160}Os and ^{156}W, Phys. Lett. B **847**, 138310 (2023).

[4] H. B. Yang, Z. G. Gan, Y. J. Li, M. L. Liu, S. Y. Xu, C. Liu, M. M. Zhang, Z. Y. Zhang, M. H. Huang, C. X. Yuan, *et al.*, Discovery of new isotopes ^{160}Os and ^{156}W: Revealing enhanced stability of the $N = 82$ shell closure on the neutron-deficient side, Phys. Rev. Lett. **132**, 072502 (2024).

[5] R. D. Page, P. J. Woods, R. A. Cunningham, T. Davinson, N. J. Davis, A. N. James, K. Livingston, P. J. Sellin, and A. C. Shotter, Radioactivity of neutron deficient isotopes in the region $N > 82 > Z$, Phys. Rev. C **53**, 660 (1996).

[6] H. Mahmud, C. N. Davids, P. J. Woods, T. Davinson, D. J. Henderson, R. J. Irvine, D. Seweryniak, and W. B. Walters, α radioactivity of ^{162}Os and ^{158}W, Phys. Rev. C **62**, 057303 (2000).

[7] D. Seweryniak, J. Uusitalo, P. Bhattacharyya, M. P. Carpenter, J. A. Cizewski, K. Y. Ding, C. N. Davids, N. Fotiades, R. V. F. Janssens, T. Lauritsen, *et al.*, Multiparticle configurations in $N = 84$ isotones located at the proton drip line, Phys. Rev. C **71**, 054319 (2005).

[8] D. T. Joss, A. Herzán, L. Donosa, J. Uusitalo, R. J. Carroll, I. G. Darby, K. Andgren, B. Cederwall, S. Eeckhaudt, T. Grahn, *et al.*, Spectroscopy at the two-proton drip line: Excited states in ^{158}W, Phys. Lett. B **772**, 703 (2017).

[9] L. Bianco, R. D. Page, I. G. Darby, D. T. Joss, J. Simpson, J. S. Al-Khalili, A. J. Cannon, B. Cederwall, S. Eeckhaudt, S. Ertürk, *et al.*, Discovery of ^{157}W and ^{161}Os, Phys. Lett. B **690**, 15 (2010).

[10] W. Reisdorf, Analysis of fissionability data at high excitation energies, Z. Phys. A **300**, 227 (1981).

[11] J. Sarén, J. Uusitalo, and H. Joukainen, In-flight recoil separators RITU and MARA and the standard detector setups, Nucl. Instrum. Methods Phys. Res. Sect. B **541**, 33 (2023).

[12] I. H. Lazarus, D. E. Appelbe, P. A. Butler, P. J. Coleman-Smith, J. R. Cresswell, S. J. Freeman, R. D. Herzberg, I. Hibbet, D. T. Joss, S. C. Letts, *et al.*, IEEE Trans. Nucl. Sci. **48**, 567 (2001).

[13] P. Rahkila, Grain—A Java data analysis system for total data readout, Nucl. Instrum. Methods Phys. Res. Sect. A **595**, 637 (2008).

[14] R. J. Carroll, R. D. Page, D. T. Joss, J. Uusitalo, I. G. Darby, K. Andgren, B. Cederwall, S. Eeckhaudt, T. Grahn, C. Gray-Jones, *et al.*, Blurring the boundaries: Decays of multiparticle isomers at the proton drip line, Phys. Rev. Lett. **112**, 092501 (2014).

[15] R. J. Carroll, R. D. Page, D. T. Joss, D. O'Donnell, J. Uusitalo, I. G. Darby, K. Andgren, K. Auranen, S. Bönig, B. Cederwall, *et al.*, Excited states in the proton-unbound nuclide ^{158}Ta, Phys. Rev. C **93**, 034307 (2016).

[16] I. G. Darby, R. D. Page, D. T. Joss, L. Bianco, T. Grahn, D. S. Judson, J. Simpson, S. Eeckhaudt, P. T. Greenlees, P. M. Jones, R. Julin, S. Juutinen, S. Ketelhut, M. Leino, A. P. Leppanen, M. Nyman, P. Rahkila, J. Saren, C. Scholey, A. N. Steer, *et al.*, Precision measurements of proton emission from the ground states of ^{156}Ta and ^{160}Re, Phys. Rev. C **83**, 064320 (2011).

[17] A. Rytz, Recommended energy and intensity values of alpha particles from radioactive decay, At. Data Nucl. Data Tables **47**, 205 (1991).

[18] R. J. Irvine, C. N. Davids, P. J. Woods, D. J. Blumenthal, L. T. Brown, L. F. Conticchio, T. Davinson, D. J. Henderson, J. A. Mackenzie, H. T. Penttilä, D. Seweryniak, and W. B. Walters, Proton emission from drip-line nuclei ^{157}Ta and ^{161}Re, Phys. Rev. C **55**, R1621(R) (1997).

[19] P. Möller, M. R. Mumpower, T. Kawano, and W. D. Myers, Nuclear properties for astrophysical and radioactive-ion-beam applications (II), At. Data Nucl. Data Tables **125**, 1 (2019).

[20] P. J. Sapple, R. D. Page, D. T. Joss, L. Bianco, T. Grahn, J. Pakarinen, J. Thomson, J. Simpson, D. O'Donnell, S. Ertürk, *et al.*, In-beam γ-ray spectroscopy of the $N = 85$ isotones ^{159}W and ^{160}Re, Phys. Rev. C **84**, 054303 (2011).

[21] D. T. Joss, I. G. Darby, R. D. Page, J. Uusitalo, S. Eeckhaudt, T. Grahn, P. T. Greenlees, P. M. Jones, R. Julin, S. Juutinen, *et al.*, Probing the limit of nuclear existence: Proton emission from ^{159}Re, Phys. Lett. B **641**, 34 (2006).

[22] R. D. Page, L. Bianco, I. G. Darby, J. Uusitalo, D. T. Joss, T. Grahn, R.-D. Herzberg, J. Pakarinen, J. Thomson, S. Eeckhaudt, P. T. Greenlees, P. M. Jones, R. Julin, S. Juutinen, S. Ketelhut, M. Leino, A. P. Leppanen, M. Nyman, P. Rahkila, and J. Saren, α decay of ^{159}Re and proton emission from ^{155}Ta, Phys. Rev. C **75**, 061302(R) (2007).

[23] R. D. Page, Limits of observable proton-emitting nuclei between the $N = 82$ and $Z = 82$ shell closures, Phys. Rev. C **83**, 014305 (2011).

[24] A. J. Sierk, Macroscopic model of rotating nuclei, Phys. Rev. C **33**, 2039 (1986).

[25] A. N. Andreyev, D. Ackermann, S. Antalic, I. G. Darby, S. Franchoo, F. P. Heßberger, S. Hofmann, M. Huyse, P. Kuusiniemi, B. Lommel, *et al.*, Cross section systematics for the lightest Bi and Po nuclei produced in complete fusion reactions with heavy ions, Phys. Rev. C **72**, 014612 (2005).

[26] K.-H. Schmidt, C.-C. Sahm, K. Pielenz, and H.-G. Clerc, Some remarks on the error analysis in the case of poor statistics, Z. Phys. A **316**, 19 (1984).

[27] G. J. Feldman and R. D. Cousins, Unified approach to the classical statistical analysis of small signals, Phys. Rev. D **57**, 3873 (1998).

[28] J. O. Rasmussen, Alpha-decay barrier penetrabilities with an exponential nuclear potential: Even-even nuclei, Phys. Rev. **113**, 1593 (1959).